

Elastic scattering susceptibility of high temperature superconductors: A comparison between a real and a momentum space spectroscopy

K. McElroy,¹ G.-H. Gweon,¹ J. Graf,¹ S. Y. Zhou,^{1,2} T. Sasagawa,^{3,4}
H. Eisaki,⁵ H. Takagi,^{3,4,6} S. Uchida,⁷ D.-H. Lee,^{1,2} and A. Lanzara^{1,2}

¹*Material Sciences Division, Lawrence Berkeley National Lab., Berkeley, CA 94720 USA*

²*Physics Department, University of California Berkeley, CA 94720 USA*

³*Department of Advanced Materials Science, University of Tokyo, Kashiwa, Chiba 277-8561, Japan*

⁴*CREST, Japan Science and Technology Agency, Saitama 332-0012, Japan*

⁵*AIST, 1-1-1 Central 2, Umezono, Tsukuba, Ibaraki, 305-8568 Japan.*

⁶*RIKEN (The Institute of Physical and Chemical Research), Wako 351-0198, Japan*

⁷*Department of Physics, University of Tokyo, Yayoi, 2-11-16 Bunkyo-ku, Tokyo 113-8656, Japan*

(Dated: December 2, 2024)

The joint density of states of $\text{Bi}_2\text{Sr}_2\text{CaCu}_2\text{O}_{8+\delta}$, a high temperature superconductor, is extracted by evaluating the autocorrelation of the single particle spectral function $A(\vec{k}, \omega)$ measured from angle resolved photoemission spectroscopy (ARPES). These results are compared with Fourier transformed conductance modulations measured by scanning tunneling microscopy. An excellent agreement between the two experimental probes is found for two different doping values examined. In addition, by changing the photon polarization, we obtained new information not accessible by Fourier transform- scanning tunneling microscopy (FT-STM) and in particular to resolve the node-node scattering vector. These results provide a new tool to directly evaluate the susceptibility of a system to elastic scattering from ARPES and provide a strong support to the joint density of states picture used to explain the spatial modulation reported by FT-STM.

Studies of quasiparticle interference have been used over the years to extract information on quasiparticle lifetime and susceptibility of a system to different scattering processes. This method has been successfully applied to a variety of materials, ranging from metals [1, 2] to semiconductors [3] and superconductors [4]. A similar approach could be extremely powerful in the case of high temperature superconductors [5], where competing orders may exist and different scattering processes have been proposed as relevant for the superconducting order.

Recently by Fourier transforming (FT) the conductance modulations due to the quasiparticle scattering measured by scanning tunneling microscopy (STM), FT-STM, distinctive patterns of peaks in the reciprocal space have been identified [6, 7, 9]. Different interpretations have been proposed in terms of quasiparticle scattering interference [6, 7, 8] and/or evidence of some type of incipient charge-order [9, 10, 13, 19].

R. Markiewicz [14] proposed a way to directly access the joint density of states (JDOS) of a material by taking advantage of the momentum space probe angle resolved photoemission spectroscopy (ARPES). This would allow access to a variety of additional information not accessible to STM today. In addition, finding a direct relationship between ARPES, a momentum space probe, and STM, a real space probe, will: 1) prove them to be consistent measures of the same underlying physical phenomenon; 2) allow for the two probes to compliment each other; 3) provide a crucial test for the JDOS model used to explain FT-STM results [6, 7, 8].

STM measures the tunneling current between a sharp tip and a clean flat surface at an energy ω , away from

the Fermi energy (E_F), and at a location \vec{r} . Within the independent tunneling approximation [12] differential conductance, $g(\vec{r}, \omega)$, is given by:

$$g(\vec{r}, \omega) = I_0 |M_{i,f}^{\vec{r}}|^2 f(\omega) A(\vec{r}, \omega) \quad (1)$$

where $M_{i,f}^{\vec{r}}$ is the tunneling matrix element, $f(\omega)$ is the Fermi function, and $A(\vec{r}, \omega)$ is the local density of states (LDOS) also known as the real space single particle spectral function. On the other hand, ARPES measures the photo current $I(\hat{e}, \vec{k}, \omega)$ ejected from a surface by UV and x-ray photons. In the sudden approximation the photo current is given by:

$$I(\hat{e}, \vec{k}, \omega) = I_0 |M_{i,f}^{\hat{e}}|^2 f(\omega) A(\vec{k}, \omega) \quad (2)$$

where $M_{i,f}^{\hat{e}}$ are the photoemission matrix elements (which depends on the photon polarization \hat{e}), $f(\omega)$ is the Fermi function, and $A(\vec{k}, \omega)$ is the momentum space single particle spectral function [20].

Within the JDOS approach the Fourier transform of the LDOS, $\rho(\vec{q}, \omega)$, is modified in the presence of an impurity by a term, $\delta\rho_1(\vec{q}, \omega)$, which is directly related to ARPES measurements of $A(\vec{k}, \omega)$ [14]:

$$\delta\rho_1(\vec{q}, \omega) = \text{Re}[\epsilon(\vec{q})] \int A(\vec{k}, \omega) A(\vec{k} + \vec{q}, \omega) d^2k, \quad (3)$$

where $\epsilon(\vec{q})$ is related to structure factor of the impurity potential. The remainder of $\delta\rho_1(\vec{q}, \omega)$ (inside the integral) is simply the autocorrelation of the ARPES (AC-ARPES) measured photocurrent, mapped over the Brillouin zone. Thus the AC-ARPES gives the susceptibility

TABLE I: Summary of samples and data reported.

T_c	$h\nu$	resolution	polarization
OPT92K	33 eV	15 meV	ΓY
UD64K	22 eV	22 meV	ΓM

of a system to scattering in the weak limit from a JDOS point of view.

Here we report the first autocorrelated ARPES (AC-ARPES) study on $\text{Bi}_2\text{Sr}_2\text{CaCu}_2\text{O}_{8+\delta}$ superconductor to calculate its elastic scattering susceptibility [15]. Data are compared with the FT-STM for two different doping values in the superconducting regime. Excellent agreement between the two probes has been obtained for energy smaller than the gap, and additional scattering vectors, not previously observed by STM have been resolved by changing the ARPES matrix element. Outside the superconducting gap, weak features along $\vec{q} \parallel (\pi, \pi)$ can still be seen, not reported by FT-STM. Our results put a strong constraint on the theories used to interpret the spatial modulations reported by FT-STM [6, 7] and provide a new tool for ARPES to directly evaluate the susceptibility of a system to elastic scattering in a complementary way to FT-STM.

The experiments were carried out at beam line 10.0.1 of the Advance Light Source of the Lawrence Berkeley National Laboratory and beam line 5.4 of the Stanford Synchrotron Radiation Laboratory. Data from two representative $\text{Bi}_2\text{Sr}_2\text{CaCu}_2\text{O}_{8+\delta}$ samples are presented here with their characteristics summarized in Table I. Both samples were measured with 0.15° angular resolution in the superconducting state at 25 K.

Figure 1a shows a map of the ARPES spectral intensity at E_F for the UD64K sample. Data were taken in one octant of the first Brillouin zone and symmetrized. The Fermi surface is identified by the highest intensity points in the spectral intensity map (black). We have used a low intensity cutoff (less than $\frac{1}{3}$ the maximum value) to suppress the contribution from the first and second order superstructure replicas. The Fermi surface shows typical arcs (banana shaped contours) near the nodal direction, ΓY and gap of spectral intensity as we approach the antinodal point M , as expected for a d-wave superconductor. In this case an additional suppression of spectral intensity can be clearly observed along the nodal direction ΓY . This is simply an effect of the ARPES matrix element[21], due to the polarization of the incoming photons parallel to the ΓM direction, in this experimental geometry. In panels b)-e) we show the autocorrelated ARPES spectra [18] for several energies below E_F . The maps exhibit distinctive patterns of peaks, which appear to disperse through the Brillouin zone as the binding energy increases. In addition we observe that, while some of these patterns remain intense, others seems to faint

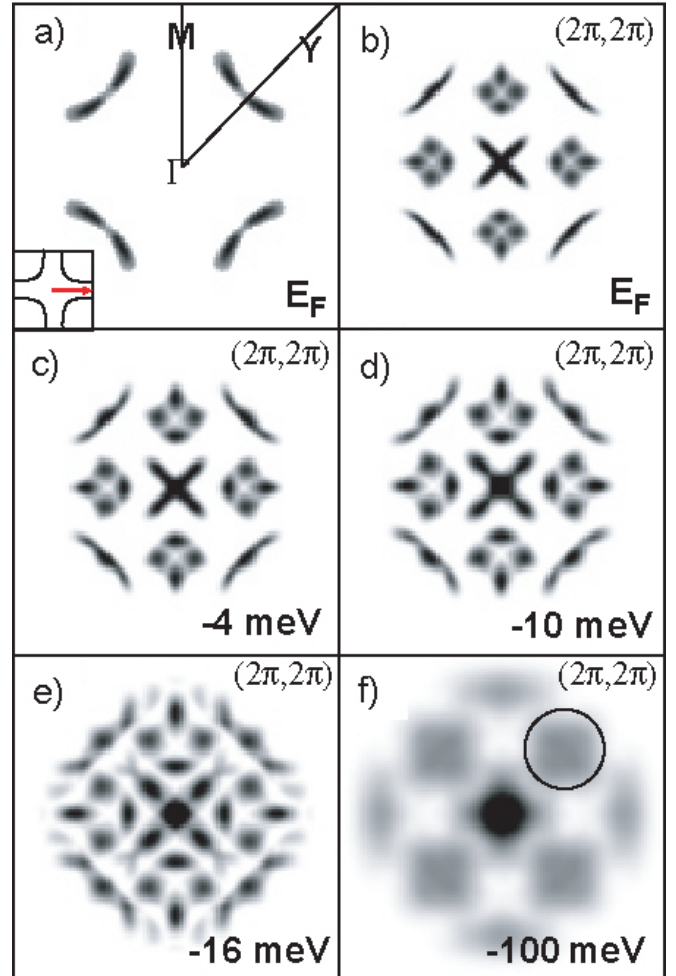


FIG. 1: a) ARPES photo current intensity measured in the octant indicated and then reflected to fill in the first Brillouin zone for the 64K UD sample. The inset shows the polarization of the incoming photons (red arrow) relative to the crystal structure. b)-e) Autocorrelations of the ARPES intensity at E_F , -4, -10, -16 meV. 32 different peaks can be seen that disperse in a systematic fashion as a function of energy. The same color scale is used in all the panels where black represent maxima of intensity and white zero intensity. f) The autocorrelation of ARPES intensity at -100 meV (outside the superconducting gap) where weak features along $\vec{q} \parallel (\pi, \pi)$ (circled) can still be seen.

out at higher binding energies.

In order to identify the nature of these peaks, as well as compare them with the FT-STM results, we show, in Figure 2, a direct comparison between the FT-STM (panel a) map [6] and AC-ARPES map (panel b) for a similar doping and energy. Circles are used to identify the peaks which are labeled accordingly to the notation used in the FT-STM data [6], where q_i are the scattering vectors associated with the elastic scattering between an ‘octet’ of well-defined Bogoliubov quasiparticles (see fig. 2 panel a) inset). Very good agreement between the two spectroscopies is observed, demonstrating the power of the AC-

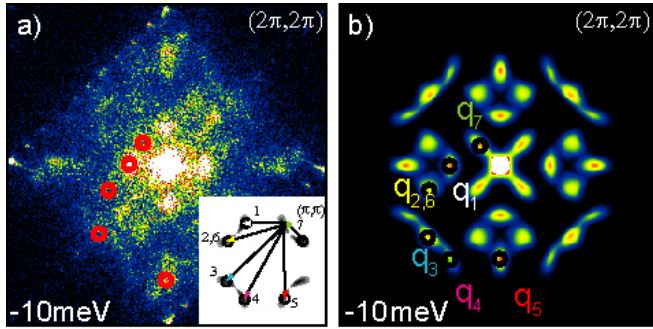


FIG. 2: a) FT-STM intensity at -10 meV adapted from [6]. Red circles mark the peaks associated with the ‘octet’ model. b) A representative AC-ARPES result at -10 meV with same peaks identified. The scattering processes and designations that result in the ‘octet’ peaks seen in these two panels are shown in the inset in panel a).

ARPES analysis. Not only most of the patterns present in the AC-ARPES map (panel b) are also observed in the FT-STM map, but also they appear to occur at the same momentum location. Additionally, agreement is also observed in the shapes of these bright patterns. For example, for q_1 or q_5 , the orientations (vertical or horizontal) of the four “cigar”-like spots is similar in both maps. Namely in both maps, the four q_1 spots look like a square when taken together, and the four q_5 spots look like a cross when taken together. These shapes come from how the banana tips overlap when autocorrelated, and nicely confirm the qualitative relevance of the auto-correlation. In the case of the AC-ARPES however, we can clearly distinguish an additional peak, q_4 , too faint to be identified by FT-STM so far, suggesting that matrix element might be relevant in determining the intensity of these peaks. We will address this point later.

This analysis can be extended to energies outside the superconducting gap energy. In particular an additional q vector $\vec{q}^* \approx (2\pi/4.5a_0, 0)$ has been reported between 65 and 150 meV in underdoped samples [19] and interpreted as evidence of a competing order parameter. Fig. 1 f) shows the AC-ARPES for a similar doping at -100 meV. Clearly there is no feature visible near this wavevector in the JDOS analysis, supporting the proposed interpretation in term of competing order [19]. Instead, a weak, previously unreported feature is here observed along $\vec{q} \parallel (\pi, \pi)$. This feature, related to P_N and circled in Fig. 1 f), would provide additional support for the JDOS model if observed in FT-STM at energies outside the gap.

To get a quantitative comparison between these results, we show in Fig. 3 cuts through the AC-ARPES data along high symmetry axes, for $q \parallel (\pi, 0)$ (panel a) and $q \parallel (\pi, \pi)$ (panel b) (for clarity the intensity was normalized so that its maximum value is unity for each curve). By following the location of the maximum position of these

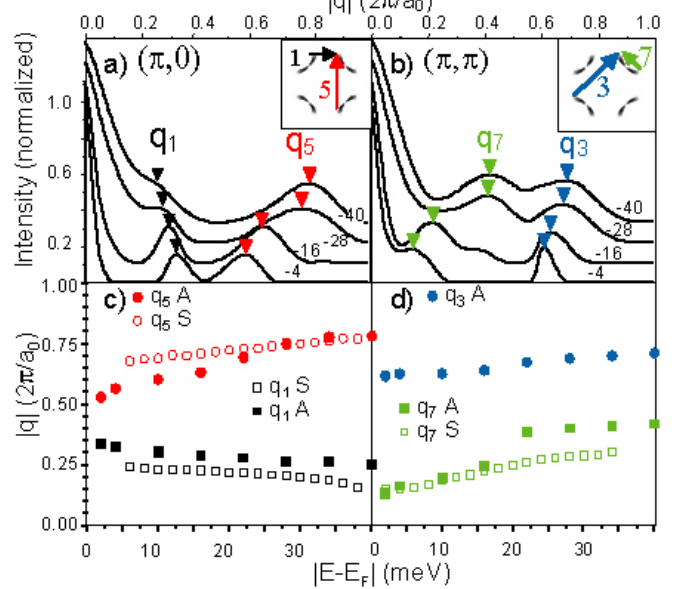


FIG. 3: a) Line cut parallel to $(\pi, 0)$ through the AC-ARPES map for several energies near the E_F , for the 64K UD sample. Dispersing peaks are indicated by triangles. b) Linecut parallel to (π, π) through the AC-ARPES map at several energies near the E_F . c) Dispersing peaks are indicated by triangles. c) Peak locations from AC-ARPES (full symbols), identified with the corresponding q -vectors from the octet model, as a function of energy for peaks in the $(\pi, 0)$ direction. Corresponding STM peaks from [19] are also plotted (empty symbols) for a similar doping. d) The same as c) but for peaks found in the (π, π) direction.

peaks as a function of energy we have extracted the dispersion relation for each of the scattering vector. The \vec{q} -vector locations are plotted in Fig. 3 c) and d) (filled symbols) for the same high symmetry axes ($q \parallel (\pi, 0)$ and $q \parallel (\pi, \pi)$ respectively), and are compared with the FT-STM results [19] for a similarly doped crystal (open symbols). Very good agreement is observed.

We note here that, within the Born limit, other terms arise which should influence the response of a system to scattering and hence the FT-STM measurements. The excellent agreement between the two probes shown here, strongly suggest that equation 3 is sufficient for finding the susceptibility of the cuprate compounds. The sufficiency of the JDOS term implies the unimportance of the off-shell, real part contribution, in agreement with theoretical calculations [8]. However, the reason for this unimportance is not obvious.

The successful comparison between the two probes clearly suggests that the interpretation in terms of scattering of Bogoliubov quasiparticle [6, 7, 8, 19] is sufficient to explain the majority of FT-STM data. However, some important differences remain to be understood. They include the observation of the q_4 scattering vector in AC-ARPES but not in FT-STM, as noted above, and simi-

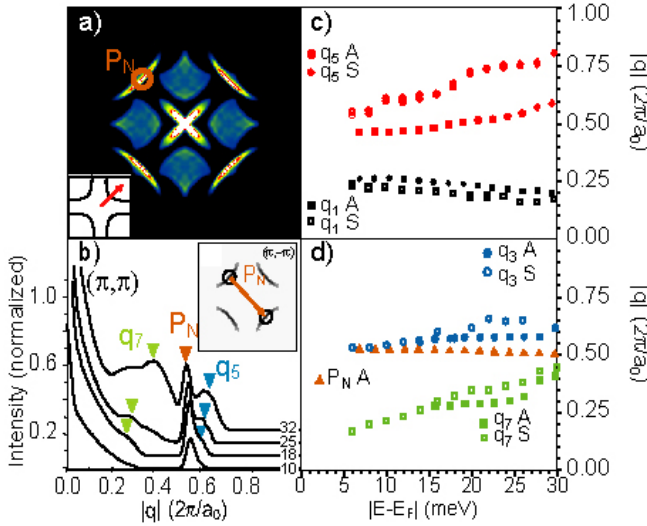


FIG. 4: a) AC-ARPES measured with the photon polarization parallel to the ΓY direction of the 92K OPT crystal. One striking difference from Fig. 1 a) is suppression of intensity along (π, π) . b) Normalized cuts along the (π, π) direction of the AC-ARPES intensity in a). Clearly the dominating feature is P_N . Small features can still be seen at the ‘octet’ wavevectors. c) Dispersions of these \vec{q} -vectors as a function of energy along $\vec{q} \parallel (\pi, 0)$. d) Dispersions of the ‘octet’ wavevectors along $\vec{q} \parallel (\pi, \pi)$ including the P_N feature.

larly the observation of a node-node scattering peak, discussed below. In particular, the absence of the latter in the FT-STM spectra has long been a puzzle, since strong nodal quasi-particle peaks are a main feature in ARPES data known in literature. Within the AC-ARPES approach, we can attribute these differences to the matrix element (see eq.’s 1,2) or elastic scattering form factor (relevant only in STM). Unfortunately, it is difficult to get any direct experimental information about these two quantities in STM alone. In contrast, by changing photon energy, or polarization, the ARPES matrix elements can be easily controlled and are well-understood[20, 21]. Thus there is an intriguing possibility now that the comparison of AC-ARPES and FT-STM can shed light on the STM matrix element and elastic scattering form factor. The former is important for interpreting STM results, while the latter can illuminate effects from competing orders which may be reflected in $\epsilon(\vec{q})$ Eqn. 3 [10, 11].

Figure 4 illustrates the effect of matrix element. In panel 4 a) we show the AC-ARPES obtained for photons with polarization \hat{e} parallel to the ΓY line (see inset panel a)) for the 92K OPT sample. In this geometry the intensity in the FS map (see inset of Fig. 4 b) is enhanced along the nodal direction with respect to the previous case (see Fig. 1). The AC-ARPES map shows bright patterns similar to the one observed in Fig. 3, but in this case the spectra are dominated by an additional bright spot, P_N . Cuts along the (π, π) direction are shown in

panel b), where the rise of the P_N peak can be clearly observed, with respect to Fig. 3 c). The dispersion of this new scattering vector is plotted in panel d) and its location makes it easy to identify it with the node-node scattering vector. The features associated with the ‘octet’ model are still evident in the AC-ARPES results for this photon polarization. Fig. 4 c) and d) show the dispersion of these \vec{q} -vectors as a function of energy below E_F , compared with the FT-STM results at the same doping. Good agreement with FT-STM is observed for this doping level (OPT92K) also. These observations not only put a strong constraint on the nature of the observed scattering processes but also provide some evidence about the form of the matrix element in STM experiments. In particular, the suppression of the node-node scattering seen in FT-STM requires a matrix element which also suppresses the states along ΓY , as recently proposed [23].

In conclusion, the AC-ARPES analysis[14] was used to calculate the elastic scattering susceptibility of $\text{Bi}_2\text{Sr}_2\text{CaCu}_2\text{O}_{8+\delta}$ for different doping values, and the results were compared to FT-STM. The excellent agreement found between the two probes provides a crucial verification of the JDOS picture [8] used to explain the density of states modulation observed in FT-STM [6, 7]. By changing the photon polarization in the AC-ARPES spectra, we were able to resolve a new scattering vector, associated with the node-node scattering, not observed by STM. In addition we also observe weak features along $\vec{q} \parallel (\pi, \pi)$ direction, outside the superconducting gap, not reported by FT-STM. These observations, predicted by the JDOS but previously not resolved in the FT-STM data, suggests that node-node scattering should be quite strong in $\text{Bi}_2\text{Sr}_2\text{CaCu}_2\text{O}_{8+\delta}$ even though STM can not see it. They also provide a new powerful tool for ARPES to directly evaluate the JDOS and allow to have access to new regimes not easily studied by STM. They also provide proof of principle for a new way to evaluate need for other order parameters in explaining the STM results[9, 10, 16] by allowing additional information about $\epsilon(\vec{q})$ to be determined.

We acknowledge and thank A. V. Balatsky, M. R. Norman, U. Chatterjee for very helpful discussions and Mr. M. Ishikado for sample growth. This work was supported by the Director, Office of Science, Office of Basic Energy Sciences, Division of Materials Sciences and Engineering of the U.S Department of Energy under Contract No. DEAC03-76SF00098; by NSF Grant No. DMR03-49361 and Grant No. DMR04-39768, the Sloan and Hellman Foundations.

-
- [1] M. F. Crommie, C. P. Lutz, D. M. Eigler, *Nature* **363**, 524 (1993).
[2] Y. Hasegawa, P. Avouris, *Phys. Rev. Let.* **71**, 1071

- (1993).
- [3] K. Kanisawa *et al.*, Phys. Rev. Lett **86**, 3384 (2001).
 - [4] A. Yazdani *et al.*, Science **275**, 1767 (1997).
 - [5] J. M. Byers, M. E. Flatté, and D. J. Scalapino, Phys. Rev. Lett. **71**, 3363 (1993).
 - [6] K. McElroy *et al.*, Nature **422**, 520 (2003).
 - [7] J. E. Hoffman *et al.*, Science **297**, 1148 (2002).
 - [8] Q.-H. Wang and D.-H. Lee, Phys. Rev. B **67**, 020511(R) (2003).
 - [9] C. Howald *et al.*, Phys. Rev. B **67**, 014533 (2003).
 - [10] Kivelson *et al.*, Rev. Modern Phys. (2004)
 - [11] D. Podolsky *et al.*, Phys. Rev. B **67**, 094514 (2003).
 - [12] Roland Wiesendanger, 1994, *Scanning Probe Microscopy and Spectroscopy*, (Cambridge University Press).
 - [13] D. Zhang, C. S. Ting, Phys. Rev. B **67**, 100506(R) (2003).
 - [14] R. S. Markiewicz, Phys. Rev. B **69**, 214517 (2004).
 - [15] During preparation of this paper we have become aware of similar work by Utpal Chatterjee *et al* submitted.
 - [16] C.-T. Chen, N.-C. Yeh, Phys. Rev. B **68**, 220505 (2003).
 - [17] H. Eisaki *et al.*, Phys. Rev. B **69** 064512, (2004).
 - [18] Backfolding in AC-ARPES was eliminated by inserting zero values into the second and third Brillouin zones.
 - [19] K. McElroy *et al.*, Phys. Rev. Lett. in press.
 - [20] Hüffner, S., 1995, *Photoelectron Spectroscopy* (Springer, Berlin).
 - [21] M. C. Asensio *et al.*, Phys. Rev. B **67**, 014519 (2003)
 - [22] L. Capriotti *et al.*, Phys. Rev. B, **68**, 014508 (2003).
 - [23] I. Martin, *et al.*, Phys. Rev. Lett. **88**, 097003 (2002).